Zwitterionic self-assembly of L-methionine nanogratings on the Ag(111) surface

Agustin Schiffrin*, Andreas Riemann*†, Willi Auwärter*, Yan Pennec*, Alex Weber-Bargioni*, Dean Cvetko‡§, Albano Cossaro§, Alberto Morgante§¶, and Johannes V. Barth*‖**

*Departments of Chemistry and of Physics and Astronomy, University of British Columbia, Vancouver, BC, Canada V6T 1Z4; †Department of Physics and Astronomy, Western Washington University, Bellingham, WA 98225; ‡Department of Physics, University of Ljubljana, SI-1001 Ljubljana, Slovenia; §Laboratorio Istituto Nazionale per la Fisica della Material/Tecnologie Avanzate e Nanoscienza (INFM/TASC), 34012 Trieste, Italy; and ¶Dipartimento di Fisica, Università di Trieste, 34127 Trieste, Italy; ‖Physik Department E20, Technische Universität München, D-85478 Garching, Germany

Edited by Royce W. Murray, University of North Carolina, Chapel Hill, NC, and approved January 11, 2007 (received for review September 8, 2006)

The engineering of complex architectures from functional molecules on surfaces provides new pathways to control matter at the nanoscale. In this article, we present a combined study addressing the self-assembly of the amino acid L-methionine on Ag(111). Scanning tunneling microscopy data reveal spontaneous ordering in extended molecular chains oriented along high-symmetry substrate directions. At intermediate coverages, regular biomolecular gratings evolve whose periodicity can be tuned at the nanometer scale by varying the methionine surface concentration. Their characteristics and stability were confirmed by helium atomic scattering. X-ray photoemission spectroscopy and high-resolution scanning tunneling microscopy data reveal that the L-methionine chaining is mediated by zwitterionic coupling, accounting for both lateral links and molecular dimerization. This methionine molecular recognition scheme is reminiscent of sheet structures in amino acid crystals and was corroborated by molecular mechanics calculations. Our findings suggest that zwitterionic assembly of amino acids represents a general construction motif to achieve biomolecular nanoarchitectures on surfaces.

nanochemistry | scanning tunneling microscopy | supramolecular engineering | surface chemistry | x-ray photoemission spectroscopy

The controlled self-assembly of functional molecular species on well defined surfaces is a promising approach toward the design of nanoscale architectures (1). By using this methodology, regular low-dimensional systems such as supramolecular clusters, chains, or nanoporous arrays can be fabricated (2–6). A wide variety of molecular species as well as substrate materials proved to be useful (7), exploiting noncovalent directional interactions including dipole–dipole coupling (2, 3), hydrogen bridges (4, 5, 8–11), and metal–ligand interactions (6, 12–15). With the exception of multiple H-bonded networks or coordination networks incorporating metal centers, it remains challenging to realize robust systems, and there is a need to develop protocols exploiting stronger intermolecular bonds to realize purely organic low-dimensional architectures. Small biological molecules such as amino acids or DNA base molecules represent an important class of building blocks that are of interest for molecular architectonic on surfaces because they inherently qualify for molecular recognition and self-assembly (16–20). The interaction between biomolecules and solid surfaces is decisive for the development of bioanalytical devices or biocompatible materials (21–23) as well as for a fundamental understanding of protein-surface bonding (24). Moreover, in three dimensions the amino acids provide assets to engineer distinct network structures based on zwitterionic coupling schemes (25–27), which may be categorized as subclass of ionic self-assembly (28), and thus are promising units to create robust nanoarchitectures. However, to date, the advantages of zwitterionic supramolecular synthons have not been exploited in two dimensions, although numerous studies on the adsorption of amino acids on metal surfaces have been performed (29).

In this article, we report a low-temperature scanning tunneling microscopy (STM) investigation on the self-assembly of L-methionine on the close-packed Ag(111) surface under ultrahigh vacuum conditions. Our results demonstrate that the interplay between both molecule–molecule and molecule–surface interactions drives a previously uncharacterized methionine self-assembly scenario. We realized extended 1D biomolecular nanostructures of distinct widths and with tunable separation controlled by the molecular surface concentration. At intermediate coverages, molecular chains form striking methionine nanogratings, which are ordered mesoscopically in micrometer domains. Complementary helium atomic scattering (HAS) observations confirm the self-assembly characteristics and the high regularity of the gratings. O 1s and N 1s x-ray photoemission spectroscopy (XPS) measurements were performed to determine the chemical nature of adsorbed L-methionine layers. They show conclusively that the organized molecules are in their zwitterionic state ($CH_3SCH_2CH_2CH(NH_3)^+(COO)^-$; for a structure model of the neutral species, see Fig. 1*a*). Molecular-resolution STM data demonstrate that the chaining reflects both a lateral coupling and a dimerization of L-methionine molecules involving the ammonium and carboxylate groups. This methionine molecular recognition scheme is steered by site-specific bonding to the silver substrate and is reminiscent of sheet structures in amino acid crystals (26, 27, 30). Elementary molecular mechanics calculations corroborate the associated 2D hydrogen-bonding pattern in which the ionic nature of the functional groups accounts for remarkably stable configurations. Because the intermolecular coupling is dominated by the amino acid functional moeities, it is expected that species with different side chains can be used in a similar manner. As such, zwitterionic assembly of amino acids represents a general motif to realize a new class of low-dimensional biomolecular nanoarchitectures.

Mesoscopic Ordering and Spectroscopic Signature

Upon deposition of small methionine concentrations, STM observations show 1D features on Ag(111) terraces, reflecting molecular self-assembly. This finding is illustrated by the image reproduced in Fig. 1*b*, taken for a coverage of ≈0.05 monolayer (ML), showing 1D arrangements with discrete widths of 19 and 38 Å, respectively. The apparent height of these structures varies between 0.8 and 1.5 Å, depending on the applied imaging bias. Moreover, they exhibit striking extensions; for instance, the

Author contributions: J.V.B. designed research; A.S., A.R., W.A., Y.P., A.W.-B., D.C., A.C., and A.M. performed research; A.S., A.R., W.A., Y.P., A.W.-B., D.C., A.C., and A.M. analyzed data; and A.S., A.R., A.M., and J.V.B wrote the paper.

The authors declare no conflict of interest.

This article is a PNAS direct submission.

Abbreviations: STM, scanning tunneling microscopy; HAS, helium atomic scattering; XPS, x-ray photoemission spectroscopy; ML, monolayer.

**To whom correspondence should be addressed. E-mail: jvb@ph.tum.de.

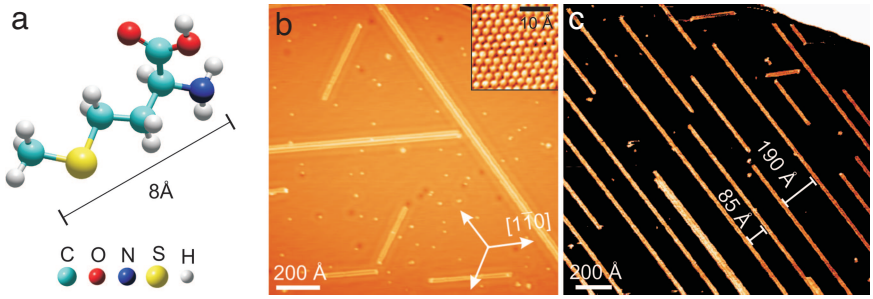

Fig. 1. The amino acid L-methionine and its 1D ordering on the Ag(111) surface. (*a*) Structure model of L-methionine in its neutral gas phase state with color-coded atoms. The length of the molecule along its side chain is ≈8 Å. (*b*) STM topographic data show the L-methionine molecules self-assembling into extended 1D arrangements following the closely packed <110> orientations of the substrate ($I = 0.7$ nA, $U = -120$ mV, $\theta \cong 0.05$ ML, $\Gamma_{evap} \cong 0.5$ ML/min). (*Inset*) Atomic resolution of Ag(111). (*c*) On exceeding a critical coverage of ≈0.1 ML, the correlated orientation of methionine stripes signals long-range repulsive interactions ($I = 0.8$ nA, $U = -200$ mV, $\theta \cong 0.12$ ML, $\Gamma_{evap} \cong 2.4$ ML/min).

length of the right 38-Å-wide methionine stripe exceeds 180 nm. Three different orientations are found that follow the close-packed <110> high-symmetry substrate orientations [see the Fig. 1*b Inset* in which the atomic structure of the Ag(111) lattice is depicted]. This is a first indication that site-specific bonding at the surface is decisive in the observed L-methionine self-assembly scenario.

The molecular surface concentration plays an important role in the mesoscopic ordering and domain formation of the molecular stripes. Although at low coverages any orientation along the close-packed substrate is equiprobable, beyond a critical coverage of ≈0.10 ML, domains with mutual alignment appear (see Fig. 1*c*), i.e., there is a mesoscopic ordering of the methionine stripes. In the data depicted in Fig. 1*c*, the interstripe distances are in the 85–190 Å range, and their correlated orientation signals long-range interactions. The nature of these presumably indirect substrate-mediated interactions is currently under investigation. The surface electronic structure, which notably includes the 2D Ag(111) surface-state free electron gas, is expected to play a preponderant role herein. Indeed, tunneling spectroscopy data evidence a striking 1D electron confinement and formation of quantum well states (31), which could mediate long-range interactions (7). Related cases in which surface-state electrons drive adatom array formation (32, 33) and influence molecular ordering (34) on metal substrates have been reported, and it is likely that with the present system the surface states interfere in the molecular self-assembly. A detailed analysis of the surface electronic structure of the present system will resolve this hypothesis.

On further increasing the coverage, the mesoscopic ordering becomes more regular. Thus, tunable and regular nanogratings can be fabricated. Fig. 2 *a* and *b* shows two corresponding examples for coverages of ≈0.15 and ≈0.38 ML, respectively. In both preparations, all stripes have a single width of 38 Å. The grating periodicity is 275 Å (standard deviation $\sigma \cong 40$ Å) in Fig. 2*a* and 94 Å ($\sigma \cong 9$ Å) in Fig. 2*b*. The nanogratings order in regular domains extending in the micrometer range. An interesting application for these nanogratings with tunable spacing is their potential use as templates for the design of functional linear arrangements such as nanowires. The thermal stability of the nanogratings has been studied by STM for this purpose, with the outcome being that they are stable up to room temperature with molecular desorption occurring only above ≈370 K.

HAS experiments confirm the linearity of the L-methionine structures and the steering influence of the substrate symmetry on the molecular nanogratings. In fact, Fig. 2*c* shows the 2D

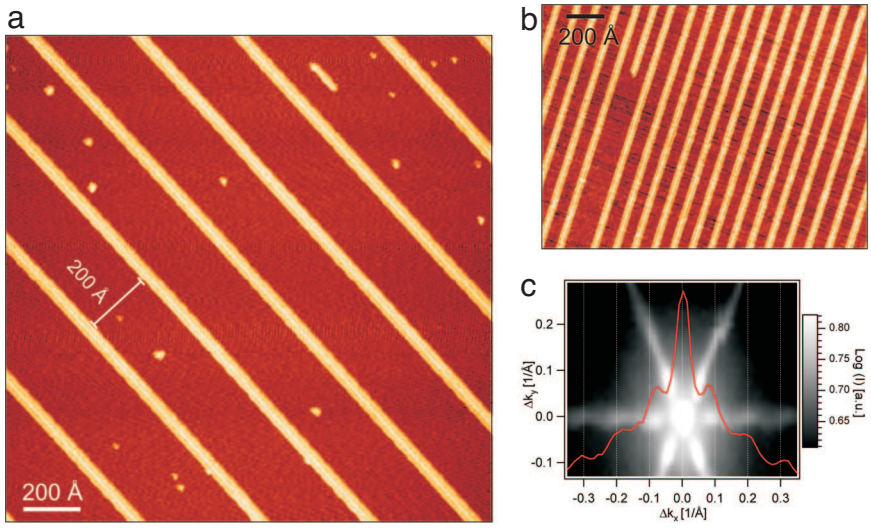

Fig. 2. Tuning the self-assembly of 1D L-methionine nanogratings at intermediate coverages. (*a*) 275 Å ($\sigma \cong 40$ Å) periodicity ($I = 0.8$ nA, $U = -800$ mV, $\theta \cong 0.15$ ML, $\Gamma_{evap} \cong 1.8$ ML/min). (*b*) 94 Å ($\sigma \cong 9$ Å) periodicity ($I = 0.1$ nA, $U = -500$ mV, $\theta \cong 0.38$ ML, $\Gamma_{evap} \cong 0.8$ ML/min). (*c*) The 2D HAS diffraction pattern of the L-methionine deposition on Ag(111) (substrate held at ≈300 K during preparation, $\theta \cong 0.6$ ML) shows the amino acid self-assembling after the sixfold symmetry of the underlying substrate. The red curve corresponds to a single scan at $\Delta k_y = 0$. Symmetrically placed satellite peaks aside the specular peak demonstrate the periodicity of the nanogratings.

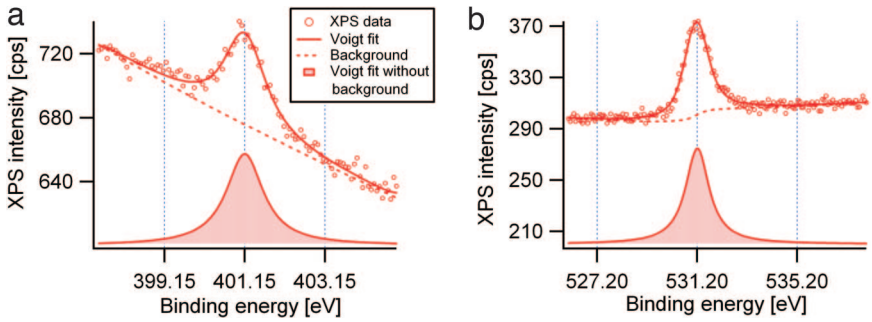

Fig. 3. XPS measurements reveal zwitterionic amino acid assemblies on Ag(111). (*a*) N 1s signal with a singular peak at $E_{N1s} = 401.15$ eV, corresponding to a NH^{+}_{3} ammonium group. (*b*) The O 1s spectrum shows only one peak at $E_{O1s} = 531.2$ eV, corresponding to the resonant oxygen atoms of the carboxylate group. Spectra were obtained for a saturated monolayer structure.

HAS diffraction pattern of the amino acid self-assembly for a 0.6-ML coverage. The hexagonal shape reflects the hexagonal symmetry of the self-assembly, induced by the close-packed Ag(111) surface. Moreover, the diffraction motif confirms that the directions in which the supramolecular structures extend correspond to the <110> substrate orientations. The periodicity of the self-assembly attributable to interchain long-range interactions also is reflected in the HAS data. The red curve in Fig. 2*c* corresponds to a single HAS scan at $\Delta k_y = 0$. The off-specular diffraction appearing as symmetrically placed satellite peaks aside the specular peak is a complementary demonstration of the periodicity of the supramolecular arrangement. Finally, HAS substantiates the room temperature stability of the gratings, which is an important feature for their potential application as templates structures (35).

XPS measurements clarify the chemical state of the amino acid moiety. These measurements were performed for a saturated monolayer preparation and are expected to apply for the entire coverage range in which the same coupling motif is identified by STM throughout (see below). The N 1s and O 1s XPS spectra in Fig. 3 *a* and *b*, respectively, show a single component at $E_{N1s} = 401.15$ eV and $E_{O1s} = 531.2$ eV, indicating a unique configuration of the amino acid. The observed energies are markedly shifted with respect to those expected for the neutral species. For comparison, XPS experiments performed on the L-cysteine/Au(110) system demonstrate that the N 1s spectra related to the neutral amino group NH_2 and the positively charged ammonium group NH_3^+ are characterized, respectively, by a peak at 399.5 eV and a peak at 401.5 eV. Moreover, the O 1s spectra of this same system show peaks at 531.2 eV, 532.3 eV, and 533.6 eV, with the first peak corresponding to the equivalent resonating oxygens of the carboxylate group COO^- and the two others corresponding to the chemically inequivalent oxygens of the neutral carboxylic group COOH (36). Therefore, we deduce that the N 1s peak at 401.15 eV of our system represents a signature of the positively charged ammonium group NH_3^+, whereas the singular maximum in the O 1s spectrum at 531.2 eV reflects the oxygen atoms of the carboxylate group COO^-, i.e., the methionine molecules are in their zwitterionic state [the slight differences in binding energy are attributed to the different substrates; note that the superstructures occurring in the adsorption of cysteine on Au(110) imply both zwitterionic coupling schemes (36, 37) and substrate reconstructions (38)]. This interpretation is in agreement with observations on the cysteine of the Pt(111) system in which similar trends are encountered (39).

Molecular-Level Observations

The high-resolution STM data in Fig. 4 reveal the L-methionine positioning within the supramolecular structures. The stripes comprise elliptical features with a long axis of 8 Å, which corresponds to the extension of a single molecule along its side chain (see Fig. 1*a*). Accordingly, these protrusions are identified with individual molecules bonding in a flat configuration to the surface. The long axis of the methionine ellipses enclose an angle of 60° ± 5° with respect to the stripe orientation (see Fig. 4*b*). Moreover, the separation between two adjacent molecules in this direction amounts to 5.8 Å. This distance corresponds to twice the Ag(111) surface lattice constant (Ag atom *nn*-distance 2.89

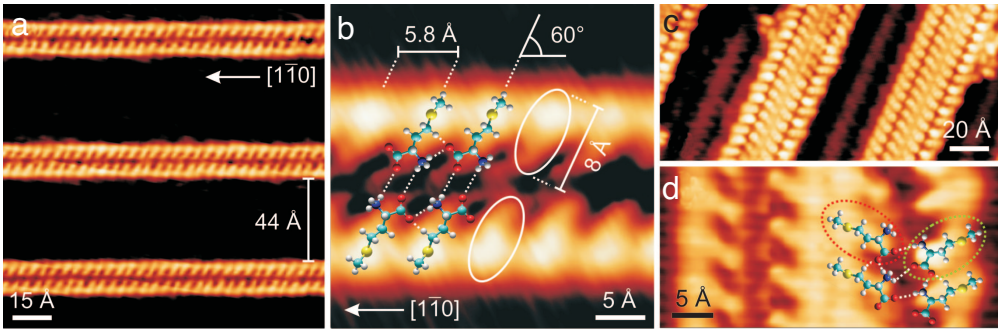

Fig. 4. Molecular resolution imaging of L-methionine stripes. (*a*) Grating of double rows with ≈63 Å periodicity ($I = 0.6$ nA, $U = -500$ mV, $\theta \cong 0.12$ ML, $\Gamma_{evap} \cong 2.4$ ML/min). (*b*) Individual molecules appear as elliptical features with a long axis of ≈8 Å arranged in pairs, with a lateral separation of 5.8 Å corresponding to twice the nearest-neighbor distance between silver surface atoms. This separation and the 60° angle of the molecules with respect to the stripe orientation reflect the influence of the substrate on the molecular self-assembly ($I = 0.9$ nA, $U = -80$ mV). (*c*) Quadruple methionine rows with 30-Å spacing. Chevron and parallel mutual row orientations coexist ($I = 0.65$ nA, $U = -1{,}100$ mV, $\theta \cong 0.50$ ML, $\Gamma_{evap} \cong 3.0$ ML/min). (*d*) Quadruple molecular row with parallel and chevron configurations. The chevron dimers correspond to a down molecule (green oval) bonded to an up molecule (red oval).

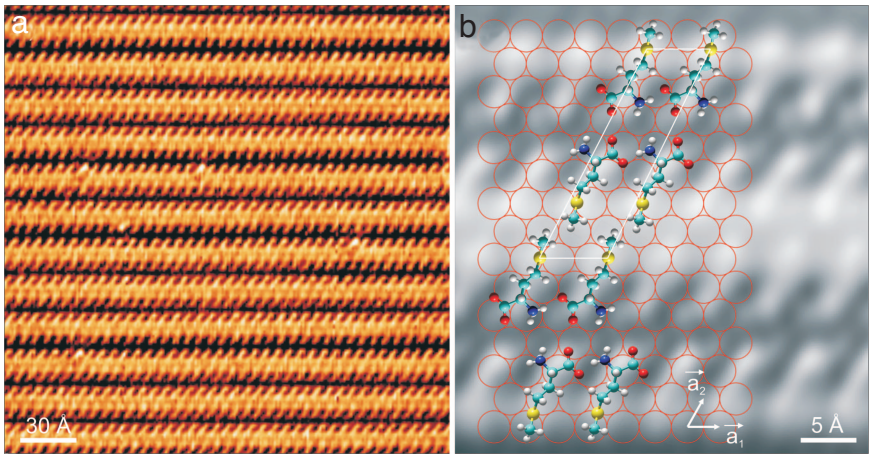

Fig. 5. Two-dimensional commensurate layer structure. (*a*) Molecular resolution imaging of saturated L-methionine monolayer (I = 0.11 nA, U = −250 mV). (*b*) Periodicity of the biomolecular self-assembly. The molecular ordering follows the atomic lattice of the Ag(111) substrate. Vectors ($\vec{a}_1$, $\vec{a}_2$) define a basis for the unit cell of the Ag(111) atomic lattice (I = 0.30 nA, U = 200 mV). The unit cell of the monolayer structure is marked in white.

Å; see Fig. 4*b*), i.e., the substrate coupling also dictates the row periodicity.

The methionine stripes forming the gratings present two discrete widths. The structures shown in Fig. 4 *a* and *c* are 19 and 38 Å wide, respectively. The molecular resolution data demonstrate that they consist of either double or quadruple molecular rows in which the methionine is oriented at specific angles with respect to the stripe direction. In both cases, the same pairing scheme of the molecules can be discerned. This finding strongly indicates that the reactive amino groups mediate dimerization. Two different molecular configurations can be observed within a dimer. Either the axis of the molecules are parallel with respect to each other or they form an angle of 120° ± 10° (chevron rows).

In Fig. 4*b*, we depict a tentative model for the parallel molecular configuration, where amino–amino dimerization and lateral coupling are accomplished through hydrogen bonding involving the ammonium and carboxylate groups. Chemical and theoretical information concerning the detailed bonding geometry at the substrate is still missing, but near-edge x-ray absorption fine-structure data show that the carboxylate group resides parallel to the surface, in agreement with the modeling. The sulfur atom also may play a secondary role in the lateral or surface bonding through its lone electron pairs. A related zwitterionic bonding scheme was identified in the formation of layered amino acid crystals, where it is associated with appreciable bonding energies (26, 30). As discussed below, this model is supported by molecular mechanics simulations. From an analysis of the molecular coupling scheme, we concluded that the bonding of the molecules is such that the H atom of the α-carbon points upward with respect to the substrate. This state is designated "up"-methionine, and its counterpart is obtained by flipping the molecule about its axis as "down"-methionine.

Fig. 4*d* depicts the molecular arrangement in the chevron configuration, which cannot be explained by the exclusive coupling of up or down species. This observation provides an intriguing possible explanation for the coexistence of the parallel and chevron rows in the nanogratings described above. The mirror symmetry of the latter with respect to the line defined by the molecular dimerization could naturally be explained by the pairing of a row of methionine molecules in the energetically preferred up configuration (circled in red in Fig. 4*d*) with another one in a down configuration (circled in green in Fig. 4*d*) being energetically close and where the lateral coupling would imply the changed orientation.

The quadruple rows correspond to a merging of two-molecule chains. Their formation cannot be explained in terms of lateral hydrogen bonding (*i*) because the terminal CH_3 group at the tail of the molecules is unreactive and (*ii*) because wider stripes composed of an even number of molecules were not found to exist at intermediate coverages. We suspect the deposition coverage θ and the deposition rate Γ_{evap} to determine whether the double or quadruple row is more favorable. Although we could not establish reliable self-assembly protocols for the respective structures, we noted that annealing methionine gratings at $T \approx 320$ K after deposition promote regular gratings with quadruple rows of up-configurated methionine. Hence, stripes of double or quadruple molecular rows are very close in energy, and the latter must be stabilized by interactions beyond direct intermolecular coupling, presumably mediated by the electronic structure or elastic response of the substrate (7).

Only with coverages exceeding ≈0.65–0.70 ML do the methionine rows merge and highly anisotropic 2D molecular islands evolve. In Fig. 5*a*, the corresponding L-methionine saturated monolayer structure is depicted. The characteristic pairing feature identified above in the molecular stripes readily is identified again. In the corresponding model depicted in Fig. 4*b*, the red circles represent the Ag(111) atomic lattice. The STM measurements do not allow for us to determine the exact adsorption sites of the molecules at the substrate. The sites on which the molecules are adsorbed in the model are arbitrary, the purpose being to determine the periodicity of the saturated molecular lattice with respect to the substrate periodicity. Considering the vectors $\vec{a}_1$, $\vec{a}_2$ that define the unit cell of the Ag(111) lattice, the lateral methionine ordering along the growth direction parallel to $\vec{a}_1$ is commensurate, whereas along $\vec{a}_2$ there is merely a higher-order commensurability. The vectors $\vec{b}_1$ and $\vec{b}_2$ defining the unit cell of the supramolecular lattice can be written as $\vec{b}_1 = 2\vec{a}_1$ and $\vec{b}_2 = -(5/2)\vec{a}_1 + (15/2)\vec{a}_2$. Hence, along the growth direction, the molecule is adsorbed at equivalent substrate sites, whereas within a given molecular dimer two molecules bond differently to the surface. Moreover, in the 2D layer, the lateral molecular ordering is strictly parallel, i.e., the chevron arrangements described above are absent. This ordering is enantiomorphic, which indicates that the chirality of the L-methionine molecule must be expressed in it. Preliminary results with the D-enantiomer confirm this hypothesis, i.e., a mirror-symmetric arrangement is found, and further studies are anticipated to identify possible related chiral resolution processes (40).

A regular chiral ordering thus is favored in the formation of extended domains to which the methionine rows come in close proximity. In agreement, the orientation of the individual molecular rows at the interior of the quadruple arrangement always was observed to be strictly parallel. This interpretation implies, assuming structures of the chevron type may form transiently in the self-assembly, that a switching of the entire orientation of the molecules with respect to the substrate is possible (from down to up), which represents a generalization of the chiral switching phenomena of specific molecular groups observed recently (41).

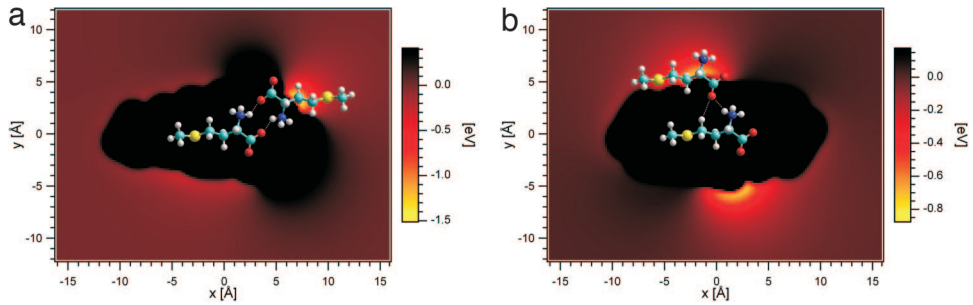

Fig. 6. Total energy maps of a system composed of two interacting L-methionine molecules obtained with molecular mechanics calculations. The origin of the 2D plots is defined by the center of mass of the immobile molecule, and *x*–*y* coordinates represent the position of the center of mass of the second molecule with respect to the immobile one. The color scale indicates total energy of the system versus the relative position between the two molecules. The energy of a noninteracting two-molecule system defines the zero of the energy scale. (*a*) Antiparallel configuration. Amino dimerization through zwitterionic bonding of self-complementary carboxylate and ammonium groups is shown. (*b*) Parallel configuration. Lateral hydrogen bonding involving ammonium and carboxylate moieties is shown.

Modeling the Zwitterionic Coupling Scheme

To gain further insight into the nature of the 2D H-bonding with the present system, molecular mechanics calculations were performed for a pair of methionine molecules confined into a plane. The classical molecular mechanics force field results lend support to the proposed model for the molecular self-assembly. Only molecule–molecule interactions were taken into account in these calculations, neglecting the influence of the Ag(111) substrate on the system, which is caused by the inaccuracy of a classical force field approach to describe surface-induced phenomena. The molecules were taken in their zwitterionic state, and conformational changes caused by molecule–molecule interactions were not considered. The STM data demonstrate that the molecules are lying flat on the substrate. If we assume that the adsorption is caused by interactions between the surface and the reactive sites of the molecules, the motion of the amino acid is restricted to the two translational degrees of freedom on the adsorption plane defined by the sulfur atom, the nitrogen atom, and one of the oxygen atoms of the carboxylate group. We considered a system composed of two L-methionine zwitterions, with their geometry independently optimized. The total energy of the system was determined with respect to the relative position of the two molecules in the adsorption plane.

Fig. 6 *a* and *b* represents total energy maps of the two-molecule system when the molecules are in antiparallel (i.e., one molecule rotated of 180° on the adsorption plane with respect to other) and parallel configurations, respectively. The origin of the maps corresponds to the center of mass of one molecule, and the coordinates are those of the center of mass of the second molecule. The first map indicates that amino dimerization involving the carboxylate and ammonium groups is energetically favorable, supporting our model. The length of the resulting dimer is 18 Å, which is in good agreement with the experimental data. The distance between a hydrogen atom of the ammonium group and an oxygen atom of the facing carboxylate group is 1.7 Å, which is in agreement with the hydrogen bond length of 3D amino acids (26). For comparison, the length of the same hydrogen bond in the tentative molecular arrangements shown in Figs. 4*b* and 5*b* is ≈3 Å, which in the calculation still is associated with appreciable bonding. However, for the superposition of the STM data, molecules in an unrelaxed configuration were used under the condition that functional moieties reside on high-symmetry positions. A possible conformational adaptation could reduce the bond length significantly. On the other hand, it is feasible that under the influence of the surface the H bond is stretched to allow for commensurability with the substrate atomic lattice (4, 42).

Furthermore, the calculation for the parallel configuration reveals that the lateral coupling proposed in our model also is energetically favorable (see Fig. 6*b*). Intermolecular bonding involving the carboxylate group and the terminating methyl group of the side chain is very weak, as expected. Here, the hydrogen bond length between an oxygen atom of the carboxylate group and a hydrogen atom of the ammonium group is 2.1 Å, whereas the hydrogen bond length between this same oxygen atom and the terminating methyl group of the side chain is 2.5 Å. All these hydrogen bonds are represented by dashed lines in Fig. 6, and the distances are in good agreement with those extracted from the tentative model based on the STM images (1.9 Å and 2.2 Å, respectively).

The combination of these results qualitatively supports our model for the molecular self-assembly and explains the formation of the double methionine rows. Furthermore, an additional stabilizing factor could result from cooperative effects, as demonstrated for example in the self-assembly of guanine on Au(111) in which resonance-assisted hydrogen bonding occurs (19). Nevertheless, the existence of quadruple rows cannot be explained in this description and is associated with substrate-mediated indirect interactions, which should be considered in further experimental or theoretical studies. Notably, the interplay between surface electronic structure and molecular self-assembly remains to be investigated in depth. Thus, further theoretical investigations are planned to explain the binding mechanism between the Ag(111) substrate and the L-methionine molecule and the resulting mesoscopic ordering in greater detail.

Concluding Remarks

In conclusion, we presented a study of the molecular self-assembly of L-methionine on the Ag(111) surface. This system provides the possibility to engineer extended biomolecular nanogratings with tunable periodicity that are mesoscopically ordered in regular domains extending in the micrometer range. The long-range linear ordering and the molecular chaining appear as a result of the molecular confinement at the surface. The driving forces underlying the observed self-assembly scenario are a combination of site-specific adsorption, zwitterionic hydrogen bonding, and long-range indirect interactions. The stability of the biomolecular superlattices, up to room temperature, coupled with their remarkable tunable geometrical characteristics make them good candidates as organic templates for the design of functional 1D nanostructures or 3D amino acid sheet structures. Because the superlattice formation exploits essentially the functionality of the amino group, the rich chemical diversity of the side chains can be exploited to realize a variety of nanogratings. Altogether, our findings suggest that zwitterionic assembly of amino acids is a general motif to realize a new class of robust molecular nanoarchitectures on surfaces.

Materials and Methods

STM measurements were performed in a custom-designed ultra-high vacuum apparatus equipped with a commercial beetle-type low-temperature STM (43) and standard tools for *in situ* sample preparation and characterization. All experiments were carried out at a base pressure lower than 3×10^{-10} mbar. The Ag(111) sample ($a_0 = 4.09$ Å at 300 K) was polished chemomechanically and prepared in ultra-high vacuum by repeated Ar^+ sputtering cycles at an energy of 0.8 keV and currents of typically 4 μA, followed by annealing at a temperature of 770 K for ≈10 min. The enantiomerically pure L-methionine molecules (≥99.5%; Sigma-Aldrich, St. Louis, MO) were vapor-deposited onto the Ag(111) substrate from a glass crucible heated to a temperature of 370 K. During deposition, the substrate was held at a temperature of ≈320 K. The methionine coverage on the silver sample was derived from STM data and is given in terms of monolayers, where 1 ML corresponds to a saturated molecular layer completely covering the surface. STM topographic images were obtained with an electrochemically etched W tip, with the bias voltage applied to the sample. Data were recorded by constant-current imaging at temperatures ≤15 K. All presented STM images were smoothed out by low-pass and inverse Fourier-transform filtering to remove, respectively, the high-frequency noise and the harmonic noise created by external vibrations. XPS and HAS measurements were performed at the ALOISA beamline (ELETTRA, Trieste, Italy), whereby deposition of L-methionine on Ag(111) was performed with the substrate held at room temperature. All XPS spectra have been measured from a freshly deposited film and by keeping the sample temperature below 150 K to minimize the radiation damage. The reported XPS spectra have been taken with an overall energy resolution of 300 meV (44) with a beam of photon energy 596.7 eV. The photon beam intensity was kept low within a reasonable noise-to-signal ratio. In fact, we observed that exposures to the synchrotron radiation beam causes molecular damage, manifested in modification of XPS peak profiles (45, 46), which can be reduced to substantially lower rates when the sample is kept below 300 K (47). The binding energy on the shown spectra was calibrated with respect to the substrate Fermi level. The XPS raw data were treated by subtracting the background signal caused by inelastically scattered photoelectrons and fitting with Voigt peaks. The HAS data were obtained at room temperature with an incident He beam of energy 19 meV and wave vector 6.3 $Å^{-1}$. For the molecular mechanics calculations, the software package HyperChem Professional 7.51 was used (Hypercube, Inc., Gainesville, FL). The optimal geometrical configuration for the isolated molecules was determined with the semiempirical MNDO/d method. The classical molecular mechanics MM+ force field was used to determine the energy of the two-methionine system.

We thank Roman Fasel for assistance with computational procedures for molecular mechanics calculations. This work was supported by the Canada Foundation of Innovation, the National Science and Engineering Research Council of Canada, and the British Columbia Knowledge Development Fund. W.A. acknowledges the Swiss National Science Foundation, and A.W.-B. acknowledges the German Academic Exchange Service for financial support.

1. Barth JV, Costantini G, Kern K (2005) *Nature* 437:671–679.
2. Böhringer M, Morgenstern K, Schneider W-D, Berndt R, Mauri F, Vita AD, Car R (1999) *Phys Rev Lett* 83:324–327.
3. Yokoyama T, Yokoyama S, Kamikado T, Okuno Y, Mashiko S (2001) *Nature* 413:619–621.
4. Barth JV, Weckesser J, Cai C, Günter P, Bürgi L, Jeandupeux O, Kern K (2000) *Angew Chem Int Ed* 39:1230–1234.
5. Theobald JA, Oxtoby NS, Phillips MA, Champness NR, Beton PH (2003) *Nature* 424:1029–1031.
6. Stepanow S, Lingenfelder M, Dmitriev A, Spillmann H, Delvigne E, Lin N, Deng X, Cai C, Barth JV, Kern K (2004) *Nature Mat* 3:229–233.
7. Barth JV (2007) *Annu Rev Phys Chem* 58:375–407.
8. Barth JV, Weckesser J, Trimarchi G, Vladimirova M, Vita AD, Cai C, Brune H, Günter P, Kern K (2002) *J Am Chem Soc* 124:7991–8000.
9. Dmitriev A, Lin N, Weckesser J, Barth JV, Kern K (2002) *J Phys Chem B* 106:6907–6912.
10. Yokoyama T, Kamikado T, Yokoyama S, Mashiko S (2004) *J Chem Phys* 121:11993–11997.
11. Miller C, Cuendet P, Grätzel M (1991) *J Phys Chem* 95:877–886.
12. Dmitriev A, Spillmann H, Lin N, Barth JV, Kern K (2003) *Angew Chem Int Ed* 41:2670–2673.
13. Clair S, Pons S, Brune H, Kern K, Barth JV (2005) *Angew Chem Int Ed* 44:7294–7297.
14. Clair S, Pons S, Fabris S, Baroni S, Brune H, Kern K, Barth JV (2006) *J Phys Chem B* 110:5627–5632.
15. Seitsonen AP, Lingenfelder M, Spillmann H, Dmitriev A, Stepanow S, Lin N, Kern K, Barth JV (2006) *J Am Chem Soc* 126:5634–5635.
16. Kawai T, Tanaka H, Nakagawa T (1997) *Surf Sci* 386:124–136.
17. Kühnle A, Linderoth TR, Hammer B, Besenbacher F (2002) *Nature* 415:891–893.
18. Chen Q, Richardson NV (2003) *Nat Mater* 2:324–328.
19. Otero R, Schöck M, Molina LM, Laegsgaard E, Stensgaard I, Hammer B, Besenbacher F (2004) *Angew Chem Int Ed* 44:2–6.
20. Kelly REA, Kantorovich LN (2006) *J Mater Chem* 16:1894–1905.
21. Kasemo B (2002) *Surf Sci* 500:656–677.
22. Sarikaya M, Tamerler C, Jen AKY, Schulten K, Baneyx F (2003) *Nat Mater* 2:577–585.
23. Preuss M, Schmidt WG, Bechstedt F (2005) *Phys Rev Lett* 94:236102.
24. Ghiringhelli LM, Schravendijk P, Sitte LD (2006) *Phys Rev B* 74:035437.
25. Schade B, Fuhrhop J-H (1998) *New J Chem* 22:97–104.
26. Dalhus B, Görbitz CH (2004) *J Mol Struct* (*Theochem*) 675:47–52.
27. Banno N, Nakanishi T, Matsunaga M, Asahi T, Osaka T (2004) *J Am Chem Soc* 126:428–429.
28. Faul CFJ, Antonietti M (2003) *Adv Mater* 15:673–683.
29. Barlow SM, Raval R (2003) *Surf Sci Rep* 50:201–341.
30. Dalhus B, Görbitz CH (1999) *Acta Crytallogr C* 55:1105–1112.
31. Pennec Y, Auwärter W, Schiffrin A, Weber-Bargioni Riemann A, Barth JV (2007) *Nature Nanotechnol* 2:99–103.
32. Merrick ML, Luo W, Fichthorn KA (2003) *Prog Surf Sci* 72:117–134.
33. Silly F, Pivetta M, Ternes M, Patthey F, Pelz JP, Schneider W-D (2004) *Phys Rev Lett* 92:16101.
34. Sykes ECH, Han P, Kandel SA, Kelly KF, McCarty GS, Weiss PS (2003) *Acc Chem Res* 36:945–953.
35. Otero R, Naitoh Y, Rosei F, Jiang P, Thostrup P, Gourdon A, Laegsgaard E, Stensgaard I, Joachim C, Besenbacher F (2004) *Angew Chem Int Ed Engl* 43:2092–2095.
36. Gonella G, Terreni S, Cvetko D, Cossaro A, Mattera L, Cavalleri O, Rolandi R, Morgante A, Floreano L, Canepa M (2005) *J Phys Chem B* 109:18003–18009.
37. Cossaro A, Terreni S, Cavalleri O, Prato M, Cvetko D, Morgante A, Floreano L, Canepa M (2006) *Langmuir* 22:11193–11198.
38. Kühnle A, Molina LM, Linderoth TR, Hammer B, Besenbacher F (2004) *Phys Rev Lett* 93:086101.
39. Löfgren P, Krozer A, Lausmaa J, Kasemo B (1997) *Surf Sci* 370:277–292.
40. Weckesser J, Vita AD, Barth JV, Cai C, Kern K (2001) *Phys Rev Lett* 87:096101.
41. Weigelt S, Busse C, Petersen L, Rauls E, Hammer B, Gothelf KV, Besenbacher F, Linderoth TR (2006) *Nat Mater* 5:112–117.
42. Clair S, Pons S, Seitsonen AP, Brune H, Kern K, Barth JV (2004) *J Phys Chem B* 108:19392–19397.
43. Meyer G (1996) *Rev Sci Instrum* 67:2960–2965.
44. Floreano L, Naletto G, Cvetko D, Gotter R, Malvezzi M, Marassi L, Morgante A, Santaniello A, Verdini A, Tommasini F, Tondello G (1999) *Rev Sci Instr* 70:3855–3864.
45. Cavalleri O, Gonella G, Terreni S, Vignolo M, Floreano L, Morgante A, Canepa M, Rolandi R (2004) *Phys Chem Chem Phys* 6:4042–4046.
46. Cavalleri O, Gonella G, Terreni S, Vignolo M, Pelori P, Floreano L, Morgante A, Canepa M, Rolandi R (2004) *J Phys Cond Matt* 16:S2477–S2482.
47. Feulner P, Niedermayer T, Eberle K, Schneider R, Menzel D, Baumer A, Schmich E, Shaporenko A, Tai Y, Zharnikov M (2004) *Phys Rev Lett* 93:178302.